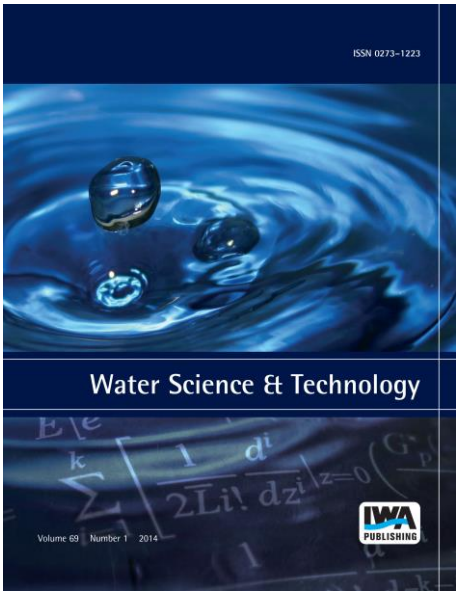

Powdered grape seeds (PGS) as an alternative biosorbent to remove pharmaceutical dyes from aqueous solutions

Gabriel Vanni, Leticia Belén Escudero and Guilherme Luiz Dotto

ABSTRACT

An alternative, low-cost and efficient biosorbent, powdered grape seeds (PGS), was prepared from wastes of a wine industry, and used to remove brilliant blue (BB) and amaranth red (AR) dyes from aqueous solutions. The biosorbent was properly characterized before and after the biosorption operation. The potential of PGS to remove BB and AR dyes was investigated thought kinetic, isotherm and thermodynamic studies. The biosorption of BB and AR was favored at pH 1.0 using biosorbent dosage of 0.500 g L^{-1}, being attained more than 85% of removal percentage. For BB and AR dyes, pseudo-second-order and Elovich models were able to explain the biosorption kinetic. The biosorption equilibrium of BB on PGS was well represented by the Langmuir model, while for AR, the Sips model was the most adequate. The maximum biosorption capacities were 599.5 and 94.2 mg g^{-1} for BB and AR, respectively. The biosorption of BB and AR on PGS was a spontaneous, favorable and endothermic process. These findings indicated that PGS is a low-cost and efficient biosorbent, which can be used to treat dye containing waters.

Key words | biosorbent, grape seeds, kinetic, pharmaceutical dyes, thermodynamic

Gabriel Vanni
Guilherme Luiz Dotto (corresponding author)
Chemical Engineering Department,
Federal University of Santa Maria,
97105-900 Santa Maria,
Brazil
E-mail: *guilherme_dotto@yahoo.com.br*

Leticia Belén Escudero
Consejo Nacional de Investigaciones Científicas y Técnicas (CONICET),
Mendoza,
Argentina
and
Laboratory of Analytical Chemistry for Research and Development (QUIANID),
Facultad de Ciencias Exactas y Naturales,
Universidad Nacional de Cuyo,
Padre J. Contreras 1300,
5500 Mendoza,
Argentina

INTRODUCTION

Dyes are commonly employed in pharmaceutical formulations to enhance the aesthetic appearance and reduce errors in medication (Pérez-Ibarbia *et al.* 2016). During the pharmaceutical manufacturing, some of these dyes are lost and, consequently, discarded in effluents (Fernández *et al.* 2010). The incorrect disposal of dye-containing effluents is a well known problem, which can cause several damages to the environment and human health (Gupta & Suhas 2009). In this way, some countries created severe restrictions for the discharge of colored effluents (Hessel *et al.* 2007) and, consequently, many studies have been focused to search for treatments able to remove dyes from aqueous effluents (Crini & Badot 2008; Álvarez *et al.* 2013; Yagub *et al.* 2014; Dotto *et al.* 2015a; Khandare & Govindwar 2015).

Several treatments are used to remove dyes from industrial effluents, including chemical precipitation, ion flotation, ion exchange, membrane filtration, AOPs, adsorption, biosorption and electrochemical methods (Yagub *et al.* 2014; Ahmed *et al.* 2017). Among these, biosorption, which is defined as 'the removal of contaminants from aqueous media by inactive or non-living biomass', has gained attention due to advantages such as low cost, ease of operation, fast kinetics and use of diverse types of biomasses as biosorbents (Dotto *et al.* 2015a). In this sense, several biosorbents have been used to remove dyes from aqueous media, for example, papaya seeds (Weber *et al.* 2014), lotus seedpod (He *et al.* 2016), spent bleaching earth (Belhaine *et al.* 2016) and oricuri fiber (Meili *et al.* 2017). The use of grape wastes has been studied in recent years. Torab-Mostaedi *et al.* (2013) verified the potential of grape peels to remove cadmium and nickel from aqueous media. Al Bsoul *et al.* (2014) studied the potential of grape seeds as biosorbent for cooper ions. In spite of these efforts, the use of grape seeds as biosorbent for dye removal is scarce.

Currently, there is a great interest in the exploitation of the residues generated by the wine industry (Spiridon *et al.* 2016; Al-Hamamre *et al.* 2017). During wine production, it is estimated that approximately 25% of the grape weight results in by-product/waste (termed 'pomace' which is comprised of skins and seeds) (Dwyer *et al.* 2014). Grape seeds contain oil, lignin, cellulose and hemicellulose (Yedro *et al.* 2015). These compounds, in turn, contain several functional groups that can act as biosorption sites. Based on this information, we believe that grape seeds can be an

doi: 10.2166/wst.2017.307

available, low cost and efficient material, that can be used as biosorbent to remove dyes from aqueous media.

In this research, an alternative low-cost and efficient biosorbent named powdered grape seeds (PGS) was prepared from wastes of a wine industry, and used to treat synthetic solutions containing the pharmaceutical dyes brilliant blue (BB) and amaranth red (AR). The biosorbent was characterized according to the point of zero charge (pH_{zpc}), Boehm titration, Fourier transform infrared spectroscopy (FT-IR), scanning electron microscopy (SEM) and energy X-ray dispersive spectroscopy (EDS). The effects of initial pH of the solution and biosorbent dosage on the biosorption were studied. The biosorption kinetic data were evaluated by the pseudo-first-order (PFO), pseudo-second-order (PSO) and Elovich models. Langmuir, Freundlich and Sips models were used to fit the biosorption equilibrium data. Thermodynamic parameters such as standard Gibbs free energy change (ΔG^0), standard enthalpy change (ΔH^0) and standard entropy change (ΔS^0) were also estimated.

MATERIALS AND METHODS

Preparation of PGS biosorbent

PGS biosorbent was prepared from wastes of a wine industry located in Mendoza, Argentina. *Vitis vinifera L.* grapes were collected from vineyards located in Mendoza province, Argentina (33°04′S, 68°19′W). The grapevine bunches (red cultivar of the *Bonarda* variety) were subjected to the wine processing. During the wine processing, a pomace containing husks, stems and seeds was generated. This pomace was refrigerated and carried to the laboratory. The grape seeds were manually separated from the pomace, washed with drinking water and then rinsed with Milli-Q water. The seeds were lyophilized for 48 h (Virtis freeze mobile, model 6, USA), pulverized with a mill (Ultracomb, MO-8100A, Argentina) and sieved until the discrete particle size ranging from 80 to 110 μm. The resulting material was named PGS biosorbent.

Characterization techniques

The PGS biosorbent was characterized according to several important aspects regarding biosorption. The point of zero charge (pH_{zpc}) was determined using the 11 points experiment (Park & Regalbuto 1995) in order to assess the surface charge of the biosorbent as a function of the pH. The total acidity and basicity of the biosorbent was verified by the Boehm titration method (Goertzen *et al.* 2010). FT-IR (Shimadzu, Prestige 21, Japan) was used to identify the main functional groups of the biosorbent (Silverstein *et al.* 2007). The textural characteristics of the biosorbent and the main elements on the surface were visualized by SEM coupled to EDS (Jeol, JSM-6610LV, Japan) (Goldstein *et al.* 1992). FT-IR and SEM were also performed after the biosorption process (optimum condition) in order to verify possible modifications on the biosorbent surface.

Pharmaceutical dyes

Two dyes commonly found in pharmaceutical effluents were selected to perform the study: BB and AR, both with industrial grade and purity higher than 85%. BB (triphenylmethane dye, molecular weight 792.8 g mol^{-1}; C.I. 42,090; $\lambda_{max} = 408$ nm) and AR (azo dye, molecular weight 604.5 g mol^{-1}; C.I. 16,185; $\lambda_{max} = 521$ nm) were supplied by a local manufacturer (Duas Rodas Ind. Jaraguá do Sul, Brazil) and were used without further purification. The three dimensional structural formulae of the dyes are shown in Figure 1. The solutions were prepared with distilled water and the reagents were of analytical grade.

Biosorption experiments

The biosorption experiments were realized in batch mode at 200 rpm using a thermostated agitator (Marconi, MA 093, Brazil) in order to verify the effects of initial pH, PGS dosage and also to obtain the kinetic and isotherm curves. Four experimental steps were performed:

- (I) The effect of initial pH was studied (from 1.0 to 8.0) (adjusted with HNO_3 and NaOH) under the following conditions: initial dye concentration of 50 mg L^{-1}, contact time of 1 h, volume of solution of 25 mL, PGS dosage of 2.00 g L^{-1} and temperature of 25 °C (PGS was put directly in contact with the solutions).
- (II) The effect of PGS dosage (from 0.25 to 5.00 g L^{-1}) was investigated under the same conditions, using the optimum pH defined elsewhere.
- (III) Kinetic experiments were performed using the optimum pH and PGS dosage defined above. The initial dye concentration was 50 mg L^{-1}. The experiments were performed at 25 °C with contact time varying from 0 to 120 min and the volume of solution was 25 mL.
- (IV) Isotherm curves were constructed at 25, 35, 45 and 55 °C, using the optimum pH and PGS dosage defined above. The initial dye concentration ranged from 25 to 300 mg L^{-1} and the volume of solution was 25 mL, with the aliquots stirred until the equilibrium (maximum 6 h).

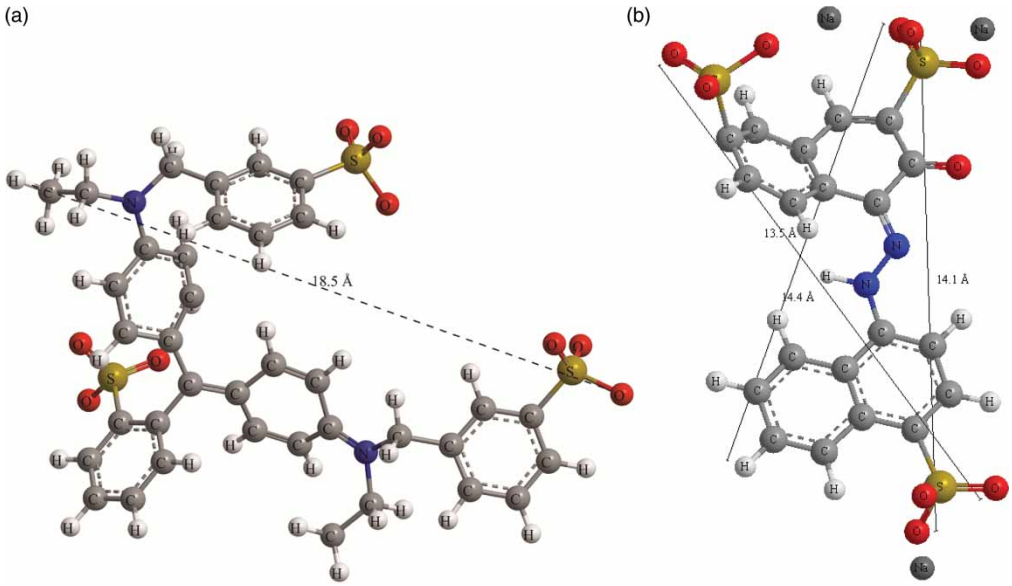

Figure 1 | Three dimensional structural formulae of the dyes: (a) BB and (b) AR.

After all the experiments, the solid phase was separated by centrifugation (Centribio, 80-2B, Brazil) at 4,000 rpm for 20 min (Dotto *et al.* 2017) and, the remaining dyes concentration in the liquid phase was measured by spectrophotometry at the maximum wavelength for each dye (Biospectro SP-22, Brazil). To guarantee the experimental accuracy, the experiments were realized in replicate ($n = 3$) using closed vessels and, blanks were performed. The dye removal percentage (R, %), mass of dye biosorbed per gram of biosorbent at any time (q_t (mg g^{-1})) and at equilibrium (q_e (mg g^{-1})) were calculated as follows (Crini & Badot 2008):

$$R = \frac{(C_0 - C_e)}{C_0} 100 \tag{1}$$

$$q_t = \frac{(C_0 - C_t)}{W} V \tag{2}$$

$$q_e = \frac{(C_0 - C_e)}{W} V \tag{3}$$

where C_o, C_t, C_e (mg L^{-1}) are the dye concentrations at $t = 0$ at any time and at equilibrium, respectively, W (g) is the biosorbent amount and V (L) is the volume of the solution.

Biosorption kinetics, isotherms and thermodynamics

The biosorption kinetics, isotherms and thermodynamics are fundamental investigations which should be performed in order to evaluate an alternative biosorbent material (Liu & Liu 2008). From the kinetic viewpoint, the biosorption of BB and AR pharmaceutical dyes on PGS was evaluated by the pseudo-first-order (Lagergren 1898), pseudo-second-order (Ho & McKay 1998) and Elovich models (Zeldowitsch 1934), as follows:

$$q_t = q_1(1 - \exp(-k_1 t)) \tag{4}$$

$$q_t = \frac{t}{(1/k_2 q_2^2) + (t/q_2)} \tag{5}$$

$$q_t = \frac{1}{b} \ln(1 + abt) \tag{6}$$

where k_1 and k_2 are the rate constants of pseudo-first-order and pseudo-second-order models, respectively, in (min^{-1}) and (g mg^{-1} min^{-1}), q_1 and q_2 are the theoretical values for the biosorption capacity (mg g^{-1}), a is the initial velocity due to dq/dt with $q_t = 0$ (mg g^{-1} min^{-1}), b is the desorption constant of the Elovich model (g mg^{-1}) and, t is the time (min).

From the equilibrium viewpoint, the BB and AR biosorption on PGS was studied using the Langmuir (Langmuir 1918), Freundlich (Freundlich 1906) and Sips (Sips 1948) isotherm models, as follows:

$$q_e = \frac{q_m K_L C_e}{1 + (K_L C_e)} \tag{7}$$

$$q_e = K_F C_e^{1/n_F} \tag{8}$$

$$q_e = \frac{q_S (K_S C_e)^m}{1 + (K_S C_e)^m} \tag{9}$$

where q_m is the maximum biosorption capacity (mg g^{-1}), K_L is the Langmuir constant (L mg^{-1}), K_F is the Freundlich constant (mg g^{-1})(mg L^{-1})$^{-1/nF}$, $1/n_F$ is the heterogeneity factor, q_S the maximum biosorption capacity from Sips

model (mg g^{-1}), K_S the Sips constant (L mg^{-1}) and m is the Sips exponent. Another important aspect of the Langmuir model is the equilibrium factor, R_L:

$$R_L = \frac{1}{1 + (K_L C_e)} \tag{10}$$

For $R_L = 1$, the isotherm is linear, $0 < R_L < 1$ indicates a favorable process and, $R_L = 0$ indicates an irreversible process (Hamdaoui & Naffrechoux 2007).

From the thermodynamic viewpoint, the biosorption of BB and AR was evaluated according to the standard values of Gibbs free energy change (ΔG^0, kJ mol^{-1}), enthalpy change (ΔH^0, kJ mol^{-1}) and entropy change (ΔS^0, kJ mol^{-1} K^{-1}), which were estimated by the combination of the following equations (Zhou *et al.* 2012; Anastopoulos & Kyzas 2016):

$$\Delta G^0 = -RT \ln (\rho K_e) \tag{11}$$

$$\Delta G^0 = \Delta H^0 - T\Delta S^0 \tag{12}$$

$$\ln(\rho K_e) = \frac{\Delta S^0}{R} - \frac{\Delta H^0}{RT} \tag{13}$$

where K_e is the equilibrium constant (L g^{-1}) (based in the parameters of the best fit isotherm model), T is the temperature (K), R is 8.31×10^{-3} kJ mol^{-1} K^{-1} and is the solution density (g L^{-1}).

Parameter estimation

The kinetic and equilibrium parameters were estimated through nonlinear regression, minimizing the least squares function and using the Quasi-Newton estimation method. The Statistic 9.1 software (Statsoft, USA) was used to perform the calculations (El-Khaiary & Malash 2011). The fit quality was measured through determination coefficient (R^2), adjusted determination coefficient (R^2_{adj}) and average relative error (ARE) (Dotto *et al.* 2013), as follows:

$$R^2 = \left(\frac{\sum_i^n (q_{i,exp} - \bar{q}_{i,exp})^2 - \sum_i^n (q_{i,exp} - q_{i,model})^2}{\sum_i^n (q_{i,exp} - \bar{q}_{i,exp})^2} \right) \tag{14}$$

$$R^2_{adj} = 1 - (1 - R^2)\left(\frac{n-1}{n-p}\right) \tag{15}$$

$$ARE = \frac{100}{n} \sum_{i=1}^{n} \left| \frac{q_{i,model} - q_{i,exp}}{q_{i,exp}} \right| \tag{16}$$

where $q_{i,model}$ is each value of q predicted by the fitted model, $q_{i,exp}$ is each value of q measured experimentally, $\bar{q}_{i,exp}$ is the average of q experimentally measured, n is the number of experimental points and p is the number of parameters.

RESULTS AND DISCUSSION

Characteristics of PGS biosorbent

PGS biosorbent was characterized according to the point of zero charge (pH_{zpc}), total acidity and basicity, FT-IR, SEM and EDS. The pH_{zpc} of the biosorbent was 6.85 (see supplementary material, available with the online version of this paper). This shows that at pH values lower than 6.85 the biosorbent is positively charged, while at pH values higher than 6.85, PGS is negatively charged. The values of carboxylic, lactonic and phenolic groups were, respectively, 0.05, 0.28 and 2.98 meq g^{-1}. Consequently, the total acidity on the PGS surface was 3.31 meq g^{-1}. The total basicity was 0.01 meq g^{-1}.

The FT-IR spectra of PGS biosorbent before (PGS) and after the biosorption process (PGS loaded BB and PGS loaded AR are depicted in Figure 2.

The PGS spectrum (before biosorption) in Figure 2 shows the main intense bands around 3,400, 2,900, 2,800, 1,750, 1,650, 1,510, 1,400 and from 1,300 to 1,000 cm^{-1}. The broad band centered at 3,400 cm^{-1} is the -OH stretching. The stretchings of C-H and CH_2 can be visualized at 2,900 and 2,800 cm^{-1}, respectively. The band at 1,750 cm^{-1} could be assigned to the carbonyl groups (C = O). The C = O link of the acetyl groups can be seen at 1,650 cm^{-1}. The C = C

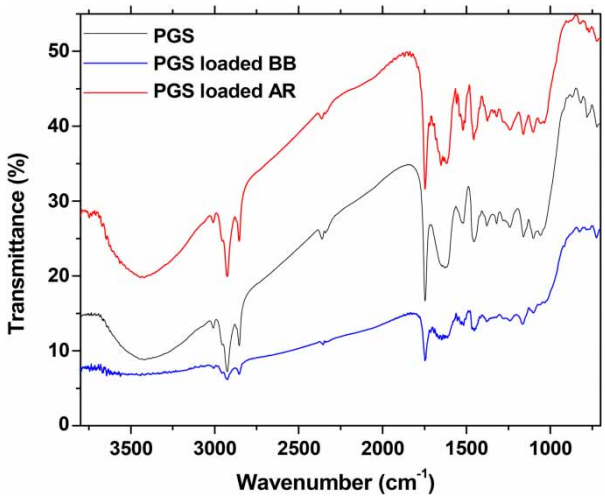

Figure 2 | FT-IR spectra of PGS biosorbent before (PGS) and after the biosorption process (PGS loaded BB and PGS loaded AR).

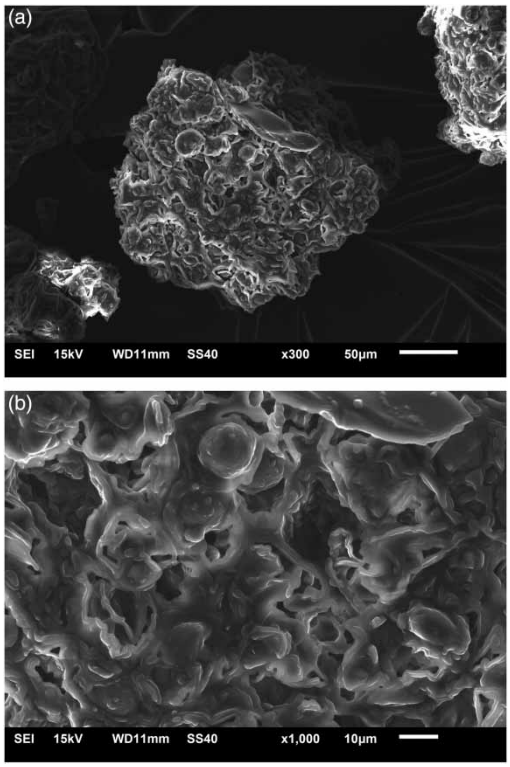

Figure 3 | SEM images of PGS biosorbent.

link of aromatic ring is visualized at 1,510 cm^{-1}. The CH deformation can be seen at 1,400 cm^{-1}. The vibrational bands in the region 1,300–1,000 cm^{-1} can be assigned to -CO, C-O-C and carboxylic acids. These bands reveal that the PGS biosorbent is composed by several functional groups that are able to bind with the pharmaceutical dyes AR and BB. In the spectra after biosorption (PGS loaded BB and PGS loaded AR) (Figure 2), no significant changes were observed. This shows that no links were formed or broken during the biosorption process, indicating that a physical biosorption occurred.

The SEM images of PGS biosorbent are presented in Figure 3. It can be seen that PGS is composed by irregular particles with a rough surface (Figure 3(a)). Figure 3(a) also confirms the mean diameter of the particles obtained by sieving (from 80 to 110 µm). Several cavities and protuberances can be also visualized in the PGS surface (Figure 3(b)). These characteristics are favorable to accommodate the large dye molecules on the biosorbent surface.

The EDS spectra of PGS biosorbent before (PGS) and after the biosorption process (PGS loaded BB and PGS loaded AR) are shown in Figure 4. It was found that the main elements on the PGS surface before the biosorption process were C, O, P and Mg. These elements are common for biosorbents. However, after the biosorption process, the element S appeared. This is indicative that BB and AR dyes (see Figure 1) were biosorbed on the PGS surface. To confirm the EDS results, PGS samples (before and after biosorption) were analyzed in an elemental analyzer (Vario E1-CHNS). The results showed that PGS before biosorption presented traces of S. However, after biosorption, the S percentage was increased. This also confirms the attachment of the dyes on the PGS surface.

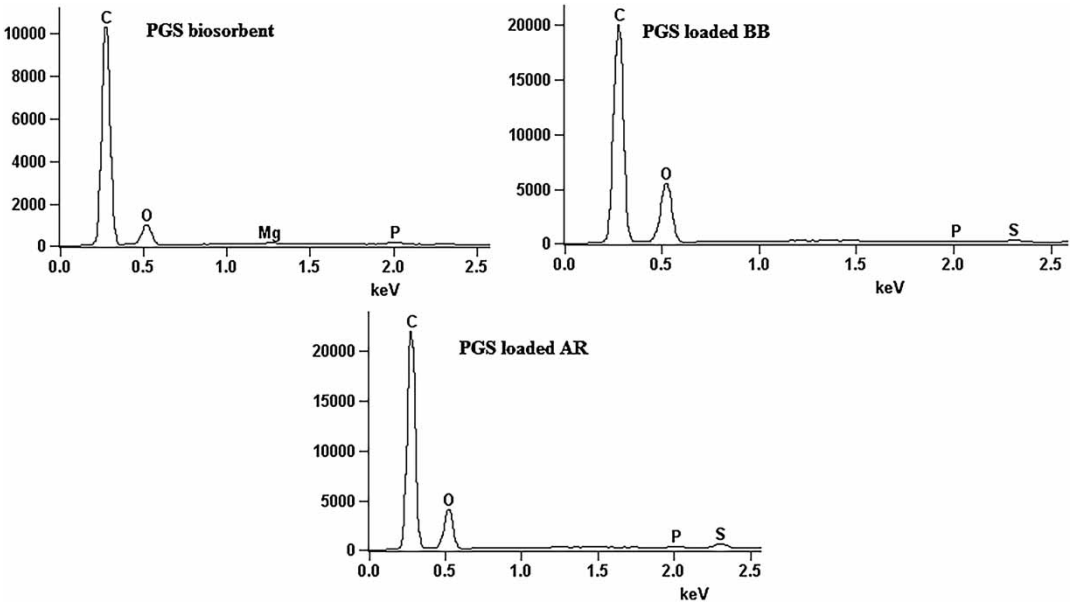

Figure 4 | EDS spectra of PGS biosorbent before (PGS) and after the biosorption process (PGS loaded BB and PGS loaded AR).

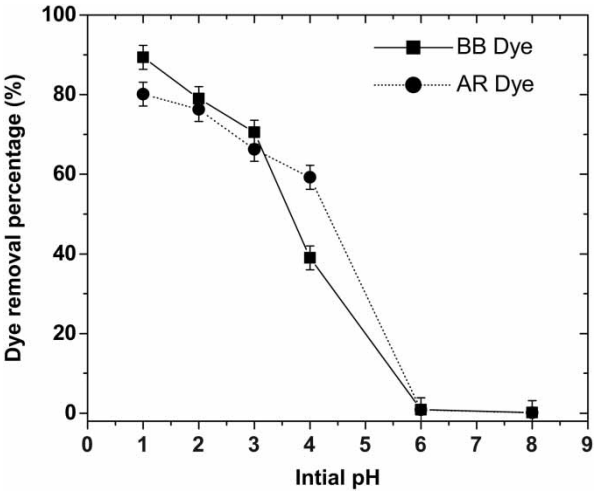

Figure 5 | Effect of initial pH on the biosorption of BB and AR dyes by PGS ($C_o = 50$ mg L^{-1}, $T = 25$ °C, $t = 1$ h, $V = 25$ mL, biosorbent dosage = 2.00 g L^{-1} and stirring rate = 200 rpm).

Effects of initial pH and biosorbent dosage

The effect of initial pH on the biosorption of BB and AR by PGS is presented in Figure 5.

It can be seen clearly in Figure 5 that the dye removal percentage increased with the pH decrease from 8.0 to 1.0. For both dyes, no biosorption occurred from pH 8.0 to 6.0, while the dye removal percentage was higher than 80% at pH 1.0. This shows that the biosorption of BB and AR dyes by PGS is strongly pH dependent. This behavior can be explained on the basis in the characteristics of the PGS and dye molecules. BB and AR are anionic dyes (Figure 1) and its sulphonated groups are negatively charged independent of the pH (since the pK_a of these groups are negative). In parallel, the PGS biosorbent is positively charged at pH values lower than 6.85 (pH_{zpc} of the biosorbent is 6.85). In this way, at pH of 1.0, the negatively charged dye molecules are attracted by the positively charged surface of the PGS biosorbent, leading to high values of removal percentage. Similar trends were found using other materials to remove BB, like chitosan (Dotto & Pinto 2011), flower wastes (Echavarria-Alvarez & Hormaza-Anaguano 2014) and *Hydrilla verticillata* (Rajeshkannan *et al.* 2011). Also, for the removal of AR using chitosan films (Cadaval *et al.* 2015), water hyacinth leaves (Guerrero-Coronilla *et al.* 2015) and tamarind pod shells (Ahalya *et al.* 2012) were used. Based on these results, the subsequent biosorption tests were performed at pH of 1.0.

The effect of biosorbent dosage on the biosorption of (a) BB and (b) AR dyes by PGS is presented in Figure 6.

For BB dye (Figure 6(a)), the increase in biosorbent dosage from 0.25 g L^{-1} to 1.00 g L^{-1} caused an increase from 56 to 87% in the dye removal percentage (R). However, the biosorption capacity (q) decreased from 120 to 40 mg g^{-1}. A new increase from 1.00 g L^{-1} to 5.00 g L^{-1} caused no significant effect on the dye removal percentage but, the biosorption capacity continued to decrease. In the case of AR dye (Figure 6(b)), the increase in biosorbent dosage from 0.25 g L^{-1} to 1.50 g L^{-1} caused an increase from 32 to 85% in the dye removal percentage (R). However, the biosorption capacity (q) decreased from 58 to 18 mg g^{-1}. A new increase from 1.50 g L^{-1} to 5.00 g L^{-1} caused no significant effect on the dye removal percentage but the biosorption capacity continued to decrease. This behavior is common, since the increase in biosorbent dosage provides more biosorption sites and, consequently, more dye is removed from the solution. On the other hand, the biosorption capacity decreases, since these additional sites can block one each other. Aiming to obtain suitable values of R and q for both

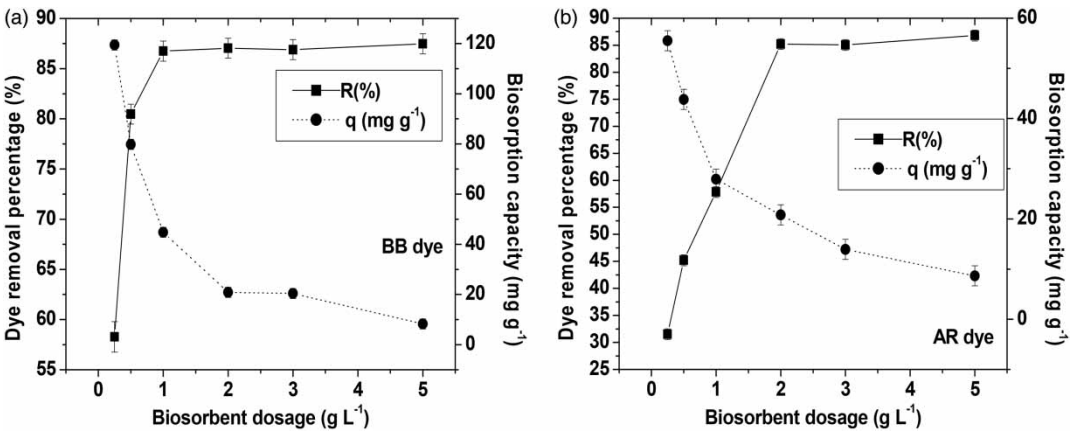

Figure 6 | Effect of biosorbent dosage on the biosorption of (a) BB and (b) AR dyes by PGS ($C_o = 50$ mg L^{-1}, $T = 25$ °C, $t = 1$ h, $V = 25$ mL, pH = 1.0 and stirring rate = 200 rpm).

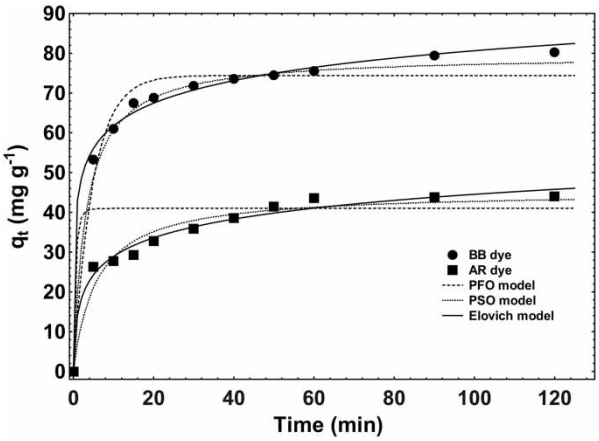

Figure 7 | Kinetic curves for the biosorption of BB and AR dyes by PGS ($C_o = 50$ mg L^{-1}, $T = 25$ °C, $V = 25$ mL, pH = 1.0, biosorbent dosage = 0.50 g L^{-1} and stirring rate = 200 rpm).

dyes, 0.50 g L^{-1} was selected as the optimum biosorbent dosage to be used in further studies.

Biosorption kinetics

The kinetic curves for the biosorption of BB and AR dyes by PGS were constructed at pH = 1.0 with biosorbent dosage of 0.50 g L^{-1}. These curves are depicted in Figure 7.

A typical kinetic behavior was observed for both dyes, where the biosorption capacity presented a strong increase in the first 5 min, followed by a gradual increase until 90 min. After, the biosorption rate decreased strongly, and the equilibrium was attained within 6 h. Also, Figure 6 shows that the biosorption capacity was higher for BB than for AR dye. This can occur because the BB molecule is higher than the AR molecule (see Figure 1), increasing the probability of this molecule being docked in an active site. This behavior was proved in other work, using physical statistics approaches (Dotto *et al.* 2015b).

PFO, PSO and Elovich models were fitted with the experimental data, in order to find an adequate and mathematically easy model to represent the experimental kinetic data. The results are presented in Table 1. The high R^2 and low *ARE* values presented in Table 1 show that the PSO and Elovich models were adequate to explain the experimental kinetic data. The q_2 value for BB was higher than the q_2 value for AR, confirming its higher biosorption capacity. This behavior is corroborated by the b parameter of the Elovich model, which was lower for BB. The k_2 values were similar for both dyes, indicating that the biosorption rate was also similar, during the entire biosorption period. However, the h_0 value was higher for BB,

Table 1 | Kinetic parameters for the biosorption of BB and AR dyes on PGS

	Dyes	
Models	**BB**	**AR**
PFO model		
q_1 (mg g^{-1})	74.4	41.0
k_1 (min^{-1})	0.207	0.113
R^2	0.9721	0.9092
ARE (%)	4.37	8.62
PSO model		
q_2 (mg g^{-1})	79.6	45.2
k_2 (g mg^{-1} min^{-1})	0.0040	0.0038
h_0 (mg g^{-1} min^{-1})	25.3	6.15
R^2	0.9959	0.9689
ARE (%)	1.73	5.66
Elovich model		
b (g mg^{-1})	0.122	0.146
a (mg g^{-1} min^{-1})	1533.13	46.69
R^2	0.9959	0.9853
ARE (%)	1.63	3.43
q_e *(exp)* (mg g^{-1})	80.2	43.9

Table 2 | Isotherm parameters for BB biosorption onto PGS

	Temperature (K)			
Models	**298**	**308**	**318**	**328**
Langmuir				
q_m (mg g^{-1})	324.4	381.6	537.3	599.5
K_L (L mg^{-1})	0.020	0.021	0.022	0.038
R_L ($C_0 = 300$ mg L^{-1})	0.131	0.142	0.136	0.080
R^2	0.9790	0.9979	0.9939	0.9985
R^2_{adj}	0.9736	0.9967	0.9918	0.9888
ARE (%)	5.91	4.18	5.76	5.54
Freundlich				
K_F ((mg g^{-1})(mg L^{-1})$^{-1/nF}$)	28.1	26.2	30.1	50.9
$1/n_F$	2.26	2.03	1.83	1.94
R^2	0.9424	0.9717	0.9757	0.9868
R^2_{adj}	0.9303	0.9656	0.9708	0.9834
ARE (%)	16.15	16.15	16.69	13.77
Sips				
q_s (mg g^{-1})	311.8	353.1	515.11	830.1
K_s (L mg^{-1})	0.025	0.024	0.023	0.017
M	1.066	1.111	1.044	0.776
R^2	0.9790	0.9970	0.9930	0.9925
R^2_{adj}	0.9676	0.9950	0.9890	0.9885
ARE (%)	7.42	5.11	5.40	6.96

indicating that, at the initial stages, the BB biosorption was faster. Finally, Table 2 shows that for both dyes, q_2 closely very well with the experimental value q_e *(exp)* confirming that the PSO model can be used to predict the experimental values of biosorption capacity.

Biosorption isotherms

Figure 8 presents the equilibrium isotherms for the biosorption of (a) BB and (b) AR dyes by PGS. For both dyes a type I isotherm (Thommes *et al.* 2015) was observed, with an initial curved portion at lower concentrations, tending to a plateau at higher concentrations. The plateau was most pronounced for AR dye. This behavior indicates a high affinity between the BB and AR molecules with the PGS surface. Furthermore, it can be seen for both dyes that the biosorption capacity increased with the temperature. This can have occurred because the temperature increase caused an expansion of the biopolymeric matrix of the biosorbent providing more available biosorption sites. Similar trend was found by Guerrero-Coronilla *et al.* (2015) in the AR adsorption onto water hyacinth leaves, using a temperature range from 18 to 50 °C.

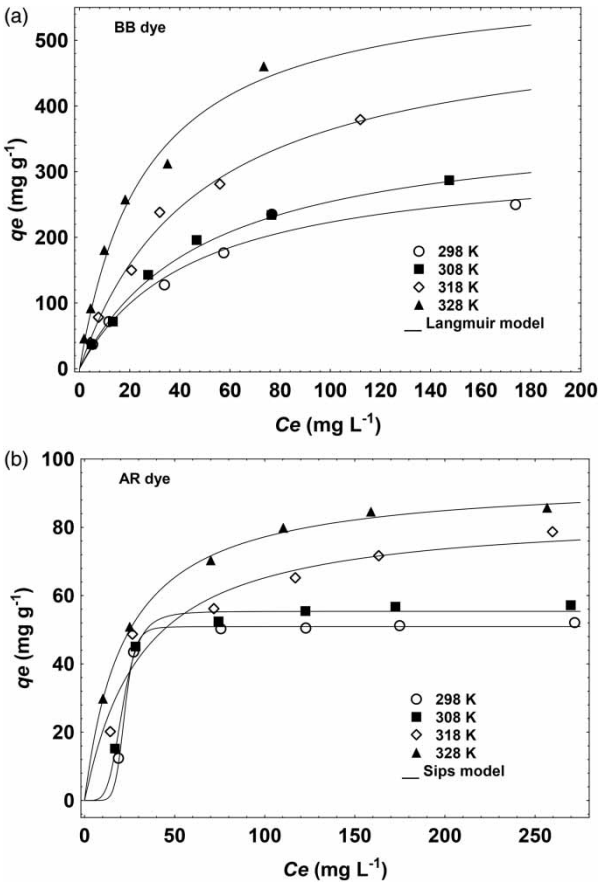

Figure 8 | Equilibrium isotherms for the biosorption of (a) BB and (b) AR dyes by PGS (pH = 1.0 and biosorbent dosage = 0.50 g L^{-1}).

In order to find an adequate representation for the equilibrium experimental data, the models named Langmuir, Freundlich and Sips were used. The fitting results are presented in Table 2 (for BB) and Table 3 (for AR). The higher values of R^2 and R^2_{adj} and the lower values of *ARE* (Table 2) indicate that the Langmuir model was the best to represent the biosorption equilibrium for the BB dye. However, for the AR dye, the Sips model was the more adequate.

The R_L values of the Langmuir model (Table 2) ranged between 0 and 1, indicating that the BB biosorption was a favorable process. The K_L (Table 2) increased with the temperature, suggesting that the biosorbent–BB affinity was higher at 328 K. The same trend was found for K_s (Table 3). The q_m (BB dye in Table 2) and q_s (AR dye in Table 3) parameters increased with the temperature, corroborating that the biosorption capacity is favored at 328 K.

The maximum biosorption capacities were found at 328 K (55 °C) and were 599.5 and 94.2 mg g^{-1} for BB and AR, respectively. A comparison between the maximum

Table 3 | Isotherm parameters for AR biosorption onto PGS

	Temperature (K)			
Models	**298**	**308**	**318**	**328**
Langmuir				
q_m (mg g^{-1})	59.8	65.6	85.6	94.4
K_L (L mg^{-1})	0.041	0.040	0.031	0.045
R_L ($C_0 = 300$ mg L^{-1})	0.075	0.076	0.097	0.068
R^2	0.8687	0.9218	0.9681	0.9981
R^2_{adj}	0.8415	0.9053	0.9613	0.9972
ARE (%)	22.77	16.04	9.29	1.16
Freundlich				
K_F ((mg g^{-1})(mg L^{-1})$^{-1/nF}$)	14.3	14.7	13.4	20.2
$1/n_F$	4.03	3.84	3.07	3.62
R^2	0.8100	0.8611	0.9493	0.9686
R^2_{adj}	0.7720	0.8332	0.9384	0.9613
ARE (%)	28.59	22.44	12.89	8.32
Sips				
q_s (mg g^{-1})	50.9	55.4	83.9	94.2
K_s (L mg^{-1})	0.045	0.047	0.033	0.048
m	7.994	4.686	1.047	1.006
R^2	0.9999	0.9957	0.9682	0.9989
R^2_{adj}	0.9988	0.9922	0.9522	0.9975
ARE (%)	0.69	1.68	9.24	1.12

Table 4 | Comparison between the maximum biosorption capacities (q_{max}) of several materials used to remove BB and AR dyes from aqueous solutions

Biosorbent	Dye	pH	T (°C)	q_{max} (mg g^{-1})	Reference
PGS	BB	1.0	55	599.5	This work
Chitosan	BB	3.0	25	210.0	Dotto & Pinto (2011)
Flower wastes	BB	2.0	54	40.16	Echavarria-Alvarez & Hormaza-Anaguano (2014)
Hydrilla verticillata	BB	3.0	30	38.46	Rajeshkannan *et al.* (2011)
Mixed sorbents	BB	3.0	30	53.6	Ho & Chiang (2001)
PGS	AR	1.0	55	94.2	This work
Chitosan films	AR	2.0	25	494.13	Cadaval *et al.* (2015)
Water hyacinth leaves	AR	2.0	18	70.0	Guerrero-Coronilla *et al.* (2015)
Tamarind pod shells	AR	2.0	–	65.04	Ahalya *et al.* (2012)
Alumina reinforced polystyrene	AR	2.0	50	20.23	Ahmad & Kumar (2011)
Activated carbon	AR	1.0	30	166.67	Al-Aoh *et al.* (2013)

biosorption capacities (q_{max}) of several materials used to remove BB and AR dyes from aqueous solutions is presented in Table 4. Based on this table, it can be stated that PGS is an excellent biosorbent to remove BB, since presented a very high biosorption capacity. Also, PGS is a suitable biosorbent for AR, since its biosorption capacity was comparable with the other materials. Furthermore, PGS has low cost, since is obtained from wastes using a simple processing.

Biosorption thermodynamics and interaction mechanism

The biosorption thermodynamic of BB and AR was evaluated according to the standard values of Gibbs free energy change (ΔG^0, kJ mol^{-1}), enthalpy change (ΔH^0, kJ mol^{-1}) and entropy change (ΔS^0, kJ mol^{-1} K^{-1}). The results are presented in Table 5.

For both dyes, negative ΔG^0 values were obtained, demonstrating that the BB and AR biosorption onto PGS was a spontaneous and favorable process. The temperature increase provided more negative ΔG^0 values, corroborating that the biosorption was favored at 328 K. The positive ΔH^0 values indicated that the biosorption was endothermic in nature. The endothermic nature was also observed in the malachite green adsorption by Moroccan clay (Elmoubarki *et al.* 2015) ($\Delta H^0 = 14.7$ kJ mol^{-1}) and reactive blue 19 adsorption on coconut shell activated carbon (Isah *et al.* 2015) ($\Delta H^0 = 7.771$ kJ mol^{-1}). For both dyes, the magnitude of ΔH^0 values suggests that physical electrostatic interactions occurred. The positive ΔS^0 values indicated some rearrangements on the biosorbent surface during the biosorption.

Based on the FT-IR, pH_{zpc}, Boehm titration, pH studies, thermodynamic parameters and dye properties, a possible main biosorption mechanism was proposed: it is known that at pH lower than 6.85, the PGS surface is positively charged. At pH 1.0, the majority of the PGS groups are protonated (basic groups, carboxylic and hydroxyl groups). In parallel, the sulphonated groups of the dye molecules are negatively charged (negative pK_a). Then a physical electrostatic interaction occurs between the dyes and the PGS biosorbent. This mechanism is corroborated by the FT-IR spectra, which were not modified after the biosorption and also by the magnitude of ΔH^0 values.

Table 5 | Thermodynamic parameters for the biosorption of BB and AR dyes on PGS

	BB dye[a]			AR dye[a]		
T (K)	ΔG^0 (kJ mol^{-1})	ΔH^0 (kJ mol^{-1})	ΔS^0 (kJ mol^{-1} K^{-1})	ΔG^0 (kJ mol^{-1})	ΔH^0 (kJ mol^{-1})	ΔS^0 (kJ mol^{-1} K^{-1})
298	−22.0 ± 0.1	30.2 ± 0.5	0.17 ± 0.02	−19.1 ± 0.1	15.0 ± 0.4	0.11 ± 0.01
308	−22.9 ± 0.1			−20.1 ± 0.1		
318	−24.6 ± 0.2			−20.9 ± 0.1		
328	−27.3 ± 0.2			−22.7 ± 0.3		

[a]Mean ± standard error.

CONCLUSION

In this work, PGS biosorbent was developed using wastes of a wine industry, and then, applied as an alternative, low cost and efficient material to remove BB and AR dyes from aqueous solutions. The material characterization revealed that PGS has potential features for biosorption, like functional groups on the surface, cavities and protuberances. The biosorption of BB and AR was favored at pH of 1.0 and biosorbent dosage of 0.50 g L^{-1}, where the dye removal percentage was higher than 80%. PSO and Elovich models were adequate to represent the biosorption kinetic. The biosorption equilibrium of BB on PGS was well represented by the Langmuir model, while for AR, the Sips model was the most adequate. The maximum biosorption capacities were 599.5 and 94.2 mg g^{-1} for BB and AR, respectively, attained at 328 K. The biosorption was a spontaneous, favorable and endothermic process. The biosorption occurred by physical electrostatic interaction between the dyes and the PGS biosorbent. These findings show that PGS is a potential candidate for biosorption purposes, since has low cost, availability, high biosorption capacity and high efficiency.

REFERENCES

Ahalya, N., Chandraprabha, M. N., Kanamadi, R. D. & Ramachandra, T. V. 2012 Adsorption of methylene blue and amaranth on to tamarind pod shells. *Journal of Biochemical Technology* **3** (5), 189–192.

Ahmad, R. & Kumar, R. 2011 Adsorption of amaranth dye onto alumina reinforced polystyrene. *Clean – Soil, Air, Water* **39** (1), 74–82.

Ahmed, M. B., Zhou, J. L., Ngo, H. H., Guo, W., Thomaidis, N. S. & Xu, J. 2017 Progress in the biological and chemical treatment technologies for emerging contaminant removal from wastewater: a critical review. *Journal of Hazardous Materials* **323** (A), 274–298.

Al-Aoh, H. A., Jamil Maah, M., Yahya, R. & Radzi Bin Abas, M. 2013 A comparative investigation on adsorption performances of activated carbon prepared from coconut husk fiber and commercial activated carbon for acid red 27 dye. *Asian Journal of Chemistry* **25** (17), 9582–9590.

Al Bsoul, A., Zeatoun, L., Abdelhay, A. & Chihad, M. 2014 Adsorption of copper ions from water by different types of natural seed materials. *Desalination and Water Treatment* **52** (31–33), 5876–5882.

Al-Hamamre, Z., Saidan, M., Hararah, M., Rawajfeh, K., Alkhasawneh, H. E. & Al-Shannag, M. 2017 Wastes and biomass materials as sustainable-renewable energy resources for Jordan. *Renewable and Sustainable Energy Reviews* **67** (1), 295–314.

Álvarez, M. S., Moscoso, F., Rodríguez, A., Sanromán, M. A. & Deive, F. J. 2013 Novel physico biological treatment for the remediation of textile dyes-containing industrial effluents. *Bioresource Technology* **146** (1), 689–695.

Anastopoulos, I. & Kyzas, G. Z. 2016 Are the thermodynamic parameters correctly estimated in liquid-phase adsorption phenomena? *Journal of Molecular Liquids* **218** (1), 174–185.

Belhaine, A., Ghezzar, M. R., Abdelmalek, F., Tayebi, K., Ghomari, A. & Addou,, A. 2016 Removal of methylene blue dye from water by a spent bleaching earth biosorbent. *Water Science & Technology* **74** (11), 2534–2540.

Cadaval Jr, T. R. S., Dotto, G. L. & Pinto, L. A. A. 2015 Equilibrium isotherms, thermodynamics, and kinetic studies for the adsorption of food azo dyes onto chitosan films. *Chemical Engineering Communications* **202** (10), 1316–1323.

Crini, G. & Badot, P. M. 2008 Application of chitosan, a natural aminopolysaccharide, for dye removal from aqueous solutions by adsorption processes using batch studies: a review of recent literature. *Progress in Polymer Science* **33** (4), 399–447.

Dotto, G. L. & Pinto, L. A. A. 2011 Adsorption of food dyes onto chitosan: optimization process and kinetic. *Carbohydrate Polymers* **84** (1), 231–238.

Dotto, G. L., Costa, J. A. V. & Pinto, L. A. A. 2013 Kinetic studies on the biosorption of phenol by nanoparticles from *Spirulina* sp. *LEB 18. Journal of Environmental Chemical Engineering* **1** (4), 1137–1143.

Dotto, G. L., Sharma, S. K. & Pinto, L. A. A. 2015a Biosorption of organic dyes: research opportunities and challenges. In: *Green Chemistry for Dyes Removal From Waste Water: Research Trends and Applications* (S. K. Sharma, ed.). John Wiley & Sons, Hoboken, NJ, USA.

Dotto, G. L., Pinto, L. A. A., Hachicha, M. A. & Knani, S. 2015b New physicochemical interpretations for the adsorption of food dyes on chitosan films using statistical physics treatment. *Food Chemistry* **171** (1), 1–7.

Dotto, G. L., Santos, J. M. N., Tanabe, E. H., Bertuol, D., Foletto, E. L., Lima, E. C. & Pavan, F. A. 2017 Chitosan/polyamide nanofibers prepared by Forcespinning® technology: a new adsorbent to remove anionic dyes from aqueous solutions. *Journal of Cleaner Production* **144** (1), 120–129.

Dwyer, K., Hosseinian, F. & Rod, M. 2014 The market potential of grape waste alternatives. *Journal of Food Research* **3** (2), 91–106.

Echavarria-Alvarez, A. M. & Hormaza-Anaguano, A. 2014 Flower wastes as a low-cost adsorbent for the removal of acid blue 9. *Dyna* **81** (185), 132–138.

El-Khaiary, M. I. & Malash, G. F. 2011 Common data analysis errors in batch adsorption studies. *Hydrometallurgy* **105** (3–4), 314–320.

Elmoubarki, R., Mahjoubi, F. Z., Tounsadi, H., Moustadraf, J., Abdennouri, M., Zouhri, A., El-Albani, A. & Barka, N. 2015 Adsorption of textile dyes on raw and decanted Moroccan clays: kinetics, equilibrium and thermodynamics. *Water Resources and Industry* **9** (1), 16–29.

Fernández, C., Larrechi, M. S. & Callao, M. P. 2010 An analytical overview of processes for removing organic dyes from

wastewater effluents. *Trends in Analytical Chemistry* **29** (10), 1202–1211.

Freundlich, H. 1906 Uber die adsorption in losungen. *Zeitschrift fur Physikalische Chemie* **57** (A), 358–471.

Goertzen, S. L., Theriault, K., Oickle, A. M., Tarasuk, A. C. & Andreas, H. A. 2010 Standardization of the Boehm titration: Part I-CO_2 expulsion and endpoint determination. *Carbon* **48** (4), 1252–1261.

Goldstein, J. I., Newbury, D. E., Echil, P., Joy, D. C., Romig Jr, A. D., Lyman, C. E., Fiori, C. & Lifshin, E. 1992 *Scanning Electron Microscopy and X-ray Microanalysis*. Plenum Press, New York, NY, USA.

Guerrero-Coronilla, I., Morales-Barrera, L. & Cristiani-Urbina, E. 2015 Kinetic, isotherm and thermodynamic studies of amaranth dye biosorption from aqueous solution onto water hyacinth leaves. *Journal of Environmental Management* **152** (1), 99–108.

Gupta, V. K. & Suhas, I. 2009 Application of low-cost adsorbents for dye removal-a review. *Journal of Environmental Management* **90** (8), 2313–2342.

Hamdaoui, O. & Naffrechoux, E. 2007 Modeling of adsorption isotherms of phenol and chlorophenols onto granular activated carbon Part I: two-parameter models and equations allowing determination of thermodynamic parameters. *Journal of Hazardous Materials* **147** (1–2), 381–394.

He, Q., Wang, H., Zhang, J., Zou, Z., Zhou, J., Yang, K. & Zheng, L. 2016 Lotus seedpod as a low-cost biomass for potential methylene blue adsorption. *Water Science & Technology* **74** (11), 2560–2568.

Hessel, C., Allegre, C., Maisseu, M., Charbit, F. & Moulin, P. 2007 Guidelines and legislation for dye house effluents. *Journal of Environmental Management* **83** (2), 171–180.

Ho, Y. S. & Chiang, C. C. 2001 Sorption studies of acid dye by mixed sorbents. *Adsorption* **7** (1), 139–147.

Ho, Y. S. & McKay, G. 1998 Kinetic models for the sorption of dye from aqueous solution by wood. *Process Safety and Environmental Protection* **76** (B2), 183–191.

Isah, U., Abdulraheem, G., Bala, S., Muhammad, S. & Abdullahi, M. 2015 Kinetics, equilibrium and thermodynamics studies of C.I. reactive blue 19 dye adsorption on coconut shell based activated carbon. *International Biodeterioration & Biodegradation* **102** (1), 265–273.

Khandare, R. V. & Govindwar, S. P. 2015 Phytoremediation of textile dyes and effluents: current scenario and future prospects. *Biotechnology Advances* **33** (8), 1697–1714.

Lagergren, S. 1898 About the theory of so-called adsorption of soluble substances. *Kungliga Svenska Vetenskapsakademiens* **24** (4), 1–39.

Langmuir, I. 1918 The adsorption of gases on plane surfaces of glass, mica and platinum. *Journal of the American Chemical Society* **40** (9), 1361–1403.

Liu, Y. & Liu, Y. J. 2008 Biosorption isotherms, kinetics and thermodynamics. *Separation and Purification Technology* **61** (3), 229–242.

Meili, L., da Silva, T. S., Henrique, D. C., Soletti, J. I., de Carvalho, S. H. V., da Silva Fonseca, E. J., de Almeida, A. R. F. & Dotto, G. L. 2017 Ouricuri (*Syagrus coronata*) fiber: a novel biosorbent to remove methylene blue from aqueous solutions. *Water Science & Technology* **75** (1), 106–114.

Park, J. & Regalbuto, J. R. 1995 A simple, accurate determination of oxide PZC and the strong buffering effect of oxide surfaces at incipient wetness. *Journal of Colloid and Interface Science* **175** (1), 239–252.

Pérez-Ibarbia, L., Majdanski, T., Schubert, S., Windhab, N. & Schuber, U. 2016 Safety and regulatory review of dyes commonly used as excipients in pharmaceutical and nutraceutical applications. *European Journal of Pharmaceutical Sciences* **93** (1), 264–273.

Rajeshkannan, R., Rajasimman, M. & Rajamohan, N. 2011 Sorption of acid blue 9 using *Hydrilla verticillata* biomass – optimization, equilibrium, and kinetics studies. *Bioremediation Journal* **15** (1), 57–67.

Silverstein, R. M., Webster,, F. X. & Kiemle,, D. J. 2007 *Spectrometric Identification of Organic Compounds*. John Wiley & Sons, New York, NY, USA.

Sips, R. 1948 On the structure of a catalyst surface. *Journal of Chemical Physics* **16** (1), 490–495.

Spiridon, I., Darie-Nita, R. N., Hitruc, G. E., Ludwiczak, J., Spiridon, I. A. C. & Niculaua, M. 2016 New opportunities to valorize biomass wastes into green materials. *Journal of Cleaner Production* **133** (1), 235–242.

Thommes, M., Kaneko, K., Neimark, A. V., Olivier, J. P., Rodriguez-Reinoso, F., Rouquerol, J. & Sing, K. S. W. 2015 Physisorption of gases, with special reference to the evaluation of surface area and pore size distribution (IUPAC Technical Report). *Pure Applied Chemistry* **87** (1), 1051–1069.

Torab-Mostaedi, M., Asadollahzadeh, M., Hemmati, A. & Khosravi, A. 2013 Equilibrium, kinetic, and thermodynamic studies for biosorption of cadmium and nickel on grapefruit peel. *Journal of the Taiwan Institute of Chemical Engineers* **44** (2), 295–302.

Weber, C. T., Collazzo, G. C., Mazutti, M. A., Foletto, E. L. & Dotto, G. L. 2014 Removal of hazardous pharmaceutical dyes by adsorption onto papaya seeds. *Water Science & Technology* **70** (1), 102–107.

Yagub, M. T., Sen, T. K., Afroze, S. & Ang, H. M. 2014 Dye and its removal from aqueous solution by adsorption: a review. *Advances in Colloid and Interface Science* **209** (1), 172–184.

Yedro, F. M., García-Serna, J., Cantero, D. A., Sobrón, F. & Cocero, M. J. 2015 Hydrothermal fractionation of grape seeds in subcritical water to produce oil extract, sugars and lignin. *Catalysis Today* **257** (2), 160–168.

Zeldowitsch, J. 1934 Über den mechanismus der katalytischen oxydation von CO an MnO_2. *Acta Physicochemical URSS* **1** (3–4), 449–464.

Zhou, X., Liu, H. & Hao, J. 2012 How to calculate the thermodynamic equilibrium constant using the Langmuir equation? *Adsorption Science & Technology* **30** (1), 647–649.

First received 19 January 2017; accepted in revised form 8 May 2017. Available online 22 May 2017